

Hybrid Stabilizing Control for the Spatial Double Inverted Pendulum

Xinjiefu, Vincent Hayward, and Hannah Michalska

Abstract The spatial double inverted pendulum actuated at the hip, but not at the foot, may be considered to be a model of standing creatures and robots. Moving in-space, as opposed to in-plane, poses new control problems which, for the most part, are still open. In this paper, a hybrid approach where an energy-shaping, passivity-based swing-up controller hands off the control to a linear-quadratic-regulator in the vicinity of the unstable upright equilibrium is proposed. A direct approach and a pre-compensated approach are described, discussed, and illustrated by means of examples in simulation.

1 Introduction

We propose that any adequate model for studying the active stabilization of articulated structures standing on a small footprint, that is not relying on torques exerted on the ground, should be spatial. The underlying motivation being that to study the stabilization of a multi-body system in the neighborhood of an unstable equilibrium, in addition to the forces due to acceleration, including gravity, the analysis should also include centrifugal and Coriolis terms. The corresponding terms entering in the system dynamics are, of course, nonlinear in essence. The simplest multi-body system that can account for these terms is the double spatial inverted pendulum which is seen in Fig. 1.

Xinjiefu and Hannah Michalska

McGill University, Department of Electrical and Computer Engineering, Montréal, Canada.
e-mail: xxinji@cim.mcgill.ca, hannah.michalska@mcgill.ca

Vincent Hayward

UPMC Univ Paris 06, UMR 7222, Institut des Systèmes Intelligents et de Robotique, Paris, France. e-mail: vincent.hayward@isir.upmc.fr

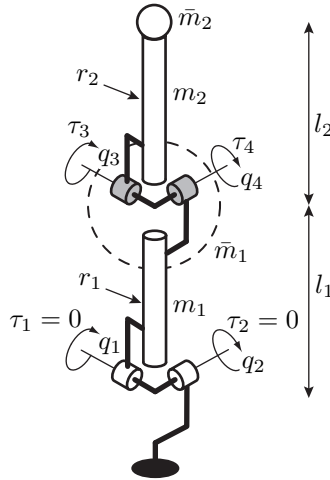


Fig. 1 Two bodies are articulated at the hip and at the ankle. Masses at the head and hip provide a plausible mass distribution for a real machine. Only the hip is actuated.

Our objective is to describe a control strategy for such systems that are characteristically underactuated and nonholonomic of order two. By the later property we mean that accelerations constraints are not integrable. The spatial double inverted pendulum is a nonlinear, underactuated mechanical system; see related works in [1, 2]. A popular approach to achieve stabilization of such systems uses swing-up control to a neighborhood of the desired equilibrium and local linear control to maintain balance within that neighborhood. The swing-up control was demonstrated for mechanical systems in the plane by using passivity results while the local linear controller can be designed by making use of one the many available techniques.

The difficulty in employing passivity-based control resides in the fact that any such design must usually be accompanied by energy shaping methods since a given energetic level of the system usually corresponds to multiple equilibria. Energy shaping not only requires a suitable storage function, but also the solution of shaping partial differential equations whose explicit solution can be very difficult. It is perhaps the reason for which passivity-based control has not yet been applied to stabilize spatial mechanical systems such as the double inverted pendulum in space. In this context, the results presented in this paper are a pioneering attempt in this direction which effectively by-passes the need for the solution of the energy shaping equations.

We first present an optimal linear controller which is effective in the neighborhood the upright unstable equilibrium. A second controller based on a hybrid energy shaping approach, is able to steer the system from a much larger set of initial conditions to a state suitably close to the unstable equilibrium where the linear controller completes the stabilization. Simulation results are presented.

2 Model of The Spatial Double Inverted Pendulum

To capture the essential kinematic and dynamic features of a standing machine, the model, Fig. 1, has two rigid cylindrical links of lengths, l_j , and radii, r_j , with masses, m_j , $j = 1, 2$, that could represent the legs and upper body of a standing machine. Additional point masses \bar{m}_1 and \bar{m}_2 are attributed to the hip and to the head. The motion of the links are restrained by universal joints at the hip and at the unactuated ankle. The derivation of the model is similar to that in [3], but is reproduced here for completeness.

2.1 Model Derivation

Taking the joints angles as generalized coordinates, $\mathbf{q} \triangleq [q_1, \dots, q_4]^\top$, in the absence of dissipation, the model is a simple Lagrangian system,

$$L(\mathbf{q}, \dot{\mathbf{q}}) = K(\mathbf{q}, \dot{\mathbf{q}}) - V(\mathbf{q}) = \frac{1}{2} \dot{\mathbf{q}}^\top \mathbf{M}(\mathbf{q}) \dot{\mathbf{q}} - V(\mathbf{q}), \quad (1)$$

where $L(\mathbf{q}, \dot{\mathbf{q}})$ is the Lagrangian function, $\mathbf{q} \in S^2 \times S^2$ is the configuration vector, and $K(\mathbf{q}, \dot{\mathbf{q}})$ and $V(\mathbf{q})$ are the kinetic and potential energies of the system, respectively. The expression for $\mathbf{M}(\mathbf{q})$ can be found in [3]. If $\mathbf{F}(\mathbf{q}) : S^2 \times S^2 \mapsto \mathbb{R}^{4 \times 2}$, represent the selection matrix of the external forces applied to the system then the Euler-Lagrange equations for the system are,

$$\frac{d}{dt} \frac{\partial L}{\partial \dot{\mathbf{q}}} - \frac{\partial L}{\partial \mathbf{q}} = \mathbf{F}(\mathbf{q}) \boldsymbol{\tau}_a,$$

where $\boldsymbol{\tau}_a \triangleq [\tau_3, \tau_4]^\top \in \mathbb{R}^2$ (subscript a means ‘‘actuated’’), and $\mathbf{F}(\mathbf{q}) = [e_3, e_4]$ where e_k is the k^{th} standard basis vector in \mathbb{R}^4 . Hence, for $k = 1, \dots, 4$, the system is governed by,

$$\sum_j m_{kj}(\mathbf{q}) \ddot{q}_j + \sum_{i,j} \Gamma_{ij}^k(\mathbf{q}) \dot{q}_i \dot{q}_j + g_k(\mathbf{q}) = e_k^\top \mathbf{F}(\mathbf{q}) \boldsymbol{\tau}_a,$$

where the gravity terms and the Christoffel symbols are given by [4],

$$g_k(\mathbf{q}) = \frac{\partial}{\partial q_k} V(\mathbf{q}), \quad \Gamma_{ij}^k(\mathbf{q}) = \frac{1}{2} \left(\frac{\partial M_{ij}(\mathbf{q})}{\partial q_k} + \frac{\partial M_{ki}(\mathbf{q})}{\partial q_j} - \frac{\partial M_{jk}(\mathbf{q})}{\partial q_i} \right). \quad (2)$$

In vector form,

$$\mathbf{M}(\mathbf{q}) \ddot{\mathbf{q}} + \dot{\mathbf{q}}^\top \mathbf{Q}(\mathbf{q}) \dot{\mathbf{q}} + G(\mathbf{q}) = \mathbf{F}(\mathbf{q}) \boldsymbol{\tau}_a, \quad (3)$$

where \mathbf{Q} is a matrix such that $\mathbf{C}(\mathbf{q}, \dot{\mathbf{q}}) \dot{\mathbf{q}} \triangleq \dot{\mathbf{q}}^\top \mathbf{Q}(\mathbf{q}) \dot{\mathbf{q}} \in \mathbb{R}^4$. The terms involving $\dot{q}_i \dot{q}_i$ represent the centrifugal forces and the terms involving $\dot{q}_i \dot{q}_j, i \neq j$,

stand for Coriolis forces. Also, $G(\mathbf{q}) = [g_1(\mathbf{q}), \dots, g_4(\mathbf{q})]^\top$ contains the gravity terms. Using (2), it is then possible to show that the matrix $\frac{d}{dt}\mathbf{M}(\mathbf{q}) - 2\mathbf{C}(\mathbf{q}, \dot{\mathbf{q}})$ is skew-symmetric. Recalling that $\mathbf{M}(\mathbf{q})$ is positive definite, hence invertible, and introducing the Legendre transformation with respect to $\dot{\mathbf{q}}$ [5],

$$\mathbf{p} = \frac{\partial L}{\partial \dot{\mathbf{q}}} = \mathbf{M}(\mathbf{q})\dot{\mathbf{q}},$$

then allows one to rewrite the system (3) in the Legendre normal form,

$$\begin{aligned}\dot{\mathbf{q}} &= \mathbf{M}^{-1}(\mathbf{q})\mathbf{p}, \\ \dot{\mathbf{p}} &= -G(\mathbf{q}) + \mathbf{p}^\top \tilde{\mathbf{Q}}(\mathbf{q})\mathbf{p} + \tilde{\mathbf{F}}(\mathbf{q})\tau_a.\end{aligned}$$

Stacking up \mathbf{q} and \mathbf{p} into $\mathbf{x} \triangleq [\mathbf{q}; \mathbf{p}]$ allows one to see that the Legendre normal form of the model takes the form of a smooth nonlinear system which is affine in the control,

$$\begin{aligned}\begin{pmatrix} \dot{\mathbf{q}} \\ \dot{\mathbf{p}} \end{pmatrix} &= \begin{pmatrix} \mathbf{M}^{-1}(\mathbf{q})\mathbf{p} \\ -G(\mathbf{q}) + \mathbf{p}^\top \tilde{\mathbf{Q}}(\mathbf{q})\mathbf{p} \end{pmatrix} + \begin{pmatrix} 0 \\ \tilde{\mathbf{F}}(\mathbf{q}) \end{pmatrix} \tau_a \\ &\triangleq \mathbf{f}(\mathbf{x}) + \mathbf{F}(\mathbf{x})\tau_a = \mathbf{f}(\mathbf{x}) + \mathbf{f}_1\tau_3 + \mathbf{f}_2\tau_4,\end{aligned}\quad (4)$$

where $\tilde{\mathbf{Q}}(\mathbf{q}) \triangleq (\mathbf{M}^{-\top}(\partial\mathbf{M}/\partial\mathbf{q} - \mathbf{Q})\mathbf{M}^{-1})(\mathbf{q})$, $\mathbf{f} : \mathbf{x} \rightarrow \mathbb{R}^8$ is the drift vector field related to the gravity field, and $\mathbf{f}_1, \mathbf{f}_2 \in \mathbb{R}^8$ are constant vector fields with $\mathbf{f}_1 = \mathbf{e}_7$ and $\mathbf{f}_2 = \mathbf{e}_8$ where \mathbf{e}_k is the k -th standard basis vector in \mathbb{R}^8 .

2.2 Model Properties

The expression for the system drift that includes the calculation of the Coriolis and centrifugal forces appearing in $\mathbf{C}(\mathbf{q}, \dot{\mathbf{q}})$ expressed through the Christoffel symbols (2) fill very many lines. It is apparent that an exact analysis of the structure of the controllability Lie algebra for the system is practically impossible as it requires the evaluation of repeated Lie brackets of the vector fields $\mathbf{f}(\mathbf{x})$, \mathbf{f}_1 , and \mathbf{f}_2 .

System (3) is underactuated with control deficiency which is determined by the difference between the rank of $\mathbf{F}(\mathbf{q})$ and the dimension of the configuration manifold. Also, the first two equations in (3) constitute a nonlinear motion constraint on the accelerations \ddot{q}_1, \ddot{q}_2 which cannot be integrated even partially, i.e., the constraints cannot be transformed into an equivalent form that contains only velocities and positions. The relation between integrability and the gravity term is discussed in [6] and [7] where sufficient conditions for integrability of second order constraints on the system accelerations are given. Non-integrability of the acceleration constraints puts the system in the category of nonholonomic systems of order two and precludes the dimen-

sion of the configuration manifold to be reduced by direct integration of the constraints. A further implication is the lack of existence of diffeomorphic state-feedback transformations that can linearize the system globally.

The local linearization of the system in the neighborhood of the unstable upright standing position, is still controllable due to the presence of the gravity term, see [6] and [7]. This allows one to consider constructing linear controllers. Nevertheless, as verified by simulations, the region of attraction for this type of stabilizing feedback is small [8, 9].

The study of small time local controllability (STLC) of the system at every configuration point away from the equilibrium would require a detailed analysis of the structure of controllability Lie algebra of the system [10].

3 Control of the spatial Double Inverted Pendulum

Since the approach adopted here is of a hybrid type, a linear controller is first constructed to stabilize the linearized system. The linear controller is able to stabilize the nonlinear system in a small neighborhood of the unstable equilibrium. Next, a nonlinear controller is designed to swing-up the system to a region of the state space from which the linear controller can take over.

3.1 LQR controller for the linearized system

Denoting $\mathbf{x} \triangleq [\mathbf{q}; \mathbf{p}]$, the linearization of (4) into $\dot{\mathbf{x}} = \mathbf{A}\mathbf{x} + \mathbf{B}\mathbf{u}$ is first derived,

$$\mathbf{A} = \left. \frac{\partial \mathbf{f}(\mathbf{x})}{\partial \mathbf{x}} \right|_{\mathbf{x}=\mathbf{0}} = \left[\begin{array}{cc} \mathbf{0} & \mathbf{M}^{-1}(\mathbf{q}) \\ -\nabla G(\mathbf{q}) & \mathbf{0} \end{array} \right] \Big|_{\mathbf{q}=\mathbf{0}, \mathbf{p}=\mathbf{0}},$$

where the matrix $\nabla G(\mathbf{q})$ is the gradient of the vector field $G(\mathbf{q})$, which is also the Hessian of the potential energy. The matrix \mathbf{B} is given by $\mathbf{B} = \mathbf{F}(\mathbf{x}) = [\mathbf{e}_7, \mathbf{e}_8]$ and the control vector is $\mathbf{u} = [\tau_3; \tau_4] = \boldsymbol{\tau}_a$. Using the following values of parameters: $m_1 = m_2 = \bar{m}_1 = \bar{m}_2 = 1.0$ kg, $l_1 = l_2 = 1.0$ m, $r_1 = r_2 = 0.1$ m, $g = 9.81$ m/s², the cost function is

$$J = \int_0^{\infty} (\mathbf{q}^\top \mathbf{Q}_1 \mathbf{q} + \mathbf{p}^\top \mathbf{Q}_2 \mathbf{p} + \boldsymbol{\tau}_a^\top \mathbf{R} \boldsymbol{\tau}_a) dt, \quad \mathbf{Q}_1 = 50 \mathbf{I}_4, \quad \mathbf{Q}_2 = \frac{1}{2} \mathbf{M}(\mathbf{0}), \quad \mathbf{R} = 100 \mathbf{I}_2.$$

Solving the algebraic Riccati equation using MATLAB delivers the following feedback law for the stabilization of the linearized system,

$$\boldsymbol{\tau}_a = \begin{pmatrix} -606 & 0 & -182 & 0 \\ 0 & -606 & 0 & -182 \end{pmatrix} \mathbf{q} - \begin{pmatrix} -37 & 0 & 17 & 0 \\ 0 & -37 & 0 & 17 \end{pmatrix} \mathbf{p}.$$

Several initial conditions were used to probe the region of convergence (ROC), see Table 1, with several initial positions of the center of mass (COM).

Table 1 Simulation results with LQR control for different initial conditions.

Example	\mathbf{q}_0^\top	$\dot{\mathbf{q}}_0^\top$	COM eccentricity	\mathbf{x}_0 in ROC
1	$[-4^\circ, 2^\circ, 8^\circ, -5^\circ]$	$\mathbf{0}$	3.69	Yes
2	$[10^\circ, -10^\circ, -30^\circ, 30^\circ]$	$\mathbf{0}$	8.26	Yes
3	$[-4^\circ, 0, 0, 0]$	$\mathbf{0}$	8.72	No
4	$[\pm 2.7^\circ, 0, 0, 0]$	$\mathbf{0}$	5.84	Yes
5	$[0, \pm 2.6^\circ, 0, 0]$	$\mathbf{0}$	5.63	Yes
6	$[0, 0, \pm 7.7^\circ, 0]$	$\mathbf{0}$	5.02	Yes
7	$[0, 0, 0, \pm 7.5^\circ]$	$\mathbf{0}$	4.89	Yes

As seen in Fig. 2a, for Example 1, the system stabilizes in about 3 seconds and in about 5 seconds for Example 2. These examples might lead to believe that the region of convergence of the LQR controller is relatively large; however, Example 3 shows that the same controller cannot stabilize the system, a fact from which we can infer that the region of convergence does not have the shape of a ball in the configuration space.

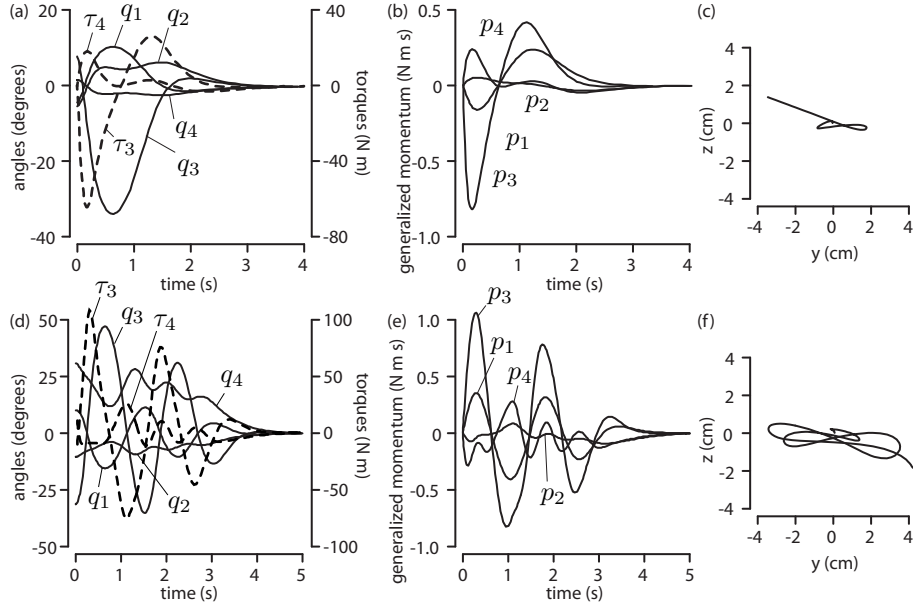


Fig. 2 LQR control Examples 1 (a,b,c) and 2 (d,e,f). a,d: Joint angles and torques through time. b,e: Generalized momenta. c,f: Stabilograms.

3.2 Energy Shaping and Passivity Based Control

The fact that the generalized inertia matrix is positive definite allows one to employ the collocated partial linearization of the system as proposed in [11]. It leads to system representation in the form of a parallel connection of sub-systems that in turn facilitates the design of passivating system outputs.

Referring to (3), the Euler-Lagrange equations of the underactuated spatial double inverted pendulum can be written,

$$\mathbf{M}_{11}(\mathbf{q})\ddot{\mathbf{q}}_u + \mathbf{M}_{12}(\mathbf{q})\ddot{\mathbf{q}}_a + C_u(\mathbf{q}, \dot{\mathbf{q}}) + G_u(\mathbf{q}) = \mathbf{0}, \quad (5)$$

$$\mathbf{M}_{21}(\mathbf{q})\ddot{\mathbf{q}}_u + \mathbf{M}_{22}(\mathbf{q})\ddot{\mathbf{q}}_a + C_a(\mathbf{q}, \dot{\mathbf{q}}) + G_a(\mathbf{q}) = \boldsymbol{\tau}_a, \quad (6)$$

where the matrices and vectors are partitioned into the actuated and unactuated parts,

$$\mathbf{M}(\mathbf{q}) = \begin{pmatrix} \mathbf{M}_{11} & \mathbf{M}_{12} \\ \mathbf{M}_{21} & \mathbf{M}_{22} \end{pmatrix}, \quad C(\mathbf{q}, \dot{\mathbf{q}})\dot{\mathbf{q}} = \begin{pmatrix} C_u(\mathbf{q}, \dot{\mathbf{q}}) \\ C_a(\mathbf{q}, \dot{\mathbf{q}}) \end{pmatrix}$$

$$G(\mathbf{q}) = \begin{pmatrix} G_u(\mathbf{q}) \\ G_a(\mathbf{q}) \end{pmatrix}, \quad \mathbf{q}_u = \begin{pmatrix} q_1 \\ q_2 \end{pmatrix}, \quad \mathbf{q}_a = \begin{pmatrix} q_3 \\ q_4 \end{pmatrix}.$$

In (5), the 2×2 block matrix $\mathbf{M}_{11}(\mathbf{q})$ is invertible, as $\mathbf{M}(\mathbf{q})$ is positive definite, thus $\ddot{\mathbf{q}}_u$ can be solved for,

$$\ddot{\mathbf{q}}_u = -\mathbf{M}_{11}^{-1}\mathbf{M}_{12}\ddot{\mathbf{q}}_a - \mathbf{M}_{11}^{-1}C_u(\mathbf{q}, \dot{\mathbf{q}}) - \mathbf{M}_{11}^{-1}G_u(\mathbf{q}) \quad (7)$$

Substituting (7) into (6) yields

$$(\mathbf{M}_{22} - \mathbf{M}_{21}\mathbf{M}_{11}^{-1}\mathbf{M}_{12})\ddot{\mathbf{q}}_a + (C_a - \mathbf{M}_{21}\mathbf{M}_{11}^{-1}C_u) + (G_a - \mathbf{M}_{21}\mathbf{M}_{11}^{-1}G_u) = \boldsymbol{\tau}_a \quad (8)$$

where the Schur complement of \mathbf{M}_{22} in $\mathbf{M}(\mathbf{q})$ is $\overline{\mathbf{M}}_{22} = \mathbf{M}_{22} - \mathbf{M}_{21}\mathbf{M}_{11}^{-1}\mathbf{M}_{12}$ and where $\overline{C}_a = C_a - \mathbf{M}_{21}\mathbf{M}_{11}^{-1}C_u$ and $\overline{G}_a = G_a - \mathbf{M}_{21}\mathbf{M}_{11}^{-1}G_u$. The matrix $\overline{\mathbf{M}}_{22}$ is positive definite since $\mathbf{M}(\mathbf{q})$ is positive definite. Eq. (8) is thus written

$$\overline{\mathbf{M}}_{22}\ddot{\mathbf{q}}_a + \overline{C}_a + \overline{G}_a = \boldsymbol{\tau}_a. \quad (9)$$

If a new control input \mathbf{v} is chosen such that,

$$\boldsymbol{\tau}_a = \overline{\mathbf{M}}_{22}\mathbf{v} + \overline{C}_a + \overline{G}_a, \quad (10)$$

then Eq. (9) is partially feedback linearized to read $\ddot{\mathbf{q}}_a = \mathbf{v}$. Together with Eq. (5), the complete system is then described by,

$$\mathbf{M}_{11}(\mathbf{q})\ddot{\mathbf{q}}_u + C_u(\mathbf{q}, \dot{\mathbf{q}}) + G_u(\mathbf{q}) = -\mathbf{M}_{12}(\mathbf{q})\mathbf{v}, \quad \ddot{\mathbf{q}}_a = \mathbf{v}, \quad (11)$$

with the new control input \mathbf{v} defined in Eq. (10). At this point, it is convenient to introduce new state variables,

$$\boldsymbol{\eta} = \begin{pmatrix} \mathbf{q}_u \\ \mathbf{q}_a \\ \dot{\mathbf{q}}_u \end{pmatrix}, \quad \mathbf{z} = \begin{pmatrix} \mathbf{q}_a \\ \dot{\mathbf{q}}_a \end{pmatrix} = \begin{pmatrix} \mathbf{z}_1 \\ \mathbf{z}_2 \end{pmatrix}.$$

Then, the second order system in (11) is expressed as a first order system,

$$\begin{aligned} \dot{\boldsymbol{\eta}} &= \boldsymbol{\omega}(\boldsymbol{\eta}) + \mathbf{h}(\boldsymbol{\eta}, \mathbf{z}) + \boldsymbol{\rho}(\boldsymbol{\eta})\mathbf{v}, & (12) \\ \dot{\mathbf{z}} &= \boldsymbol{\Phi}\mathbf{z} + \boldsymbol{\Psi}\mathbf{v}, & (13) \end{aligned}$$

where the linearized sub-system that represents two double integrators has state space matrices, $\boldsymbol{\Phi} = \begin{pmatrix} \mathbf{0} & \mathbf{I} \\ \mathbf{0} & \mathbf{0} \end{pmatrix}$, $\boldsymbol{\Psi} = (\mathbf{0} \ \mathbf{I})$, and where the functions $\boldsymbol{\omega}(\boldsymbol{\eta})$, $\mathbf{h}(\boldsymbol{\eta}, \mathbf{z})$, $\boldsymbol{\rho}(\boldsymbol{\eta})$ are defined by,

$$\begin{aligned} \boldsymbol{\omega}(\boldsymbol{\eta}) &= \begin{pmatrix} \dot{\mathbf{q}}_u \\ \mathbf{0} \\ -\mathbf{M}_{11}^{-1}(G_u(\mathbf{q}) + \tilde{C}_u(\mathbf{q}, \dot{\mathbf{q}}_u)\dot{\mathbf{q}}_u) \end{pmatrix}, \\ \mathbf{h}(\boldsymbol{\eta}, \mathbf{z}) &= \begin{pmatrix} \mathbf{0} \\ \dot{\mathbf{q}}_a \\ -\mathbf{M}_{11}^{-1}\tilde{C}_u(\mathbf{q}, \dot{\mathbf{q}}) \end{pmatrix}, \quad \boldsymbol{\rho}(\boldsymbol{\eta}) = \begin{pmatrix} \mathbf{0} \\ \mathbf{0} \\ -\mathbf{M}_{11}^{-1}\mathbf{M}_{12} \end{pmatrix}. \end{aligned}$$

Since the vector $C_u(\mathbf{q}, \dot{\mathbf{q}})$ is a quadratic function of $\dot{\mathbf{q}}$, it can be decomposed into a sum of two terms, $C_u(\mathbf{q}, \dot{\mathbf{q}}) = \tilde{C}_u(\mathbf{q}, \dot{\mathbf{q}}_u)\dot{\mathbf{q}}_u + \hat{C}_u(\mathbf{q}, \dot{\mathbf{q}})$, where the first term, $\tilde{C}_u(\mathbf{q}, \dot{\mathbf{q}}_u)\dot{\mathbf{q}}_u$, contains the quadratic terms in $\dot{\mathbf{q}}_u$, and the second term, $\hat{C}_u(\mathbf{q}, \dot{\mathbf{q}})$, contains the cross terms involving both $\dot{\mathbf{q}}_u$ and $\dot{\mathbf{q}}_a$ and also the quadratic terms in $\dot{\mathbf{q}}_a$. We conclude that

$$\mathbf{h}(\boldsymbol{\eta}, \mathbf{0}) = \mathbf{0}.$$

Introducing the energy-like function associated with the η -sub-system as

$$E_\eta = \frac{1}{2}\dot{\mathbf{q}}_u^\top \mathbf{M}_{11}(\mathbf{q})\dot{\mathbf{q}}_u + V(\mathbf{q}),$$

it is easy to verify that its time derivative is given by

$$\begin{aligned} \dot{E}_\eta &= \frac{\partial E_\eta}{\partial \boldsymbol{\eta}} \dot{\boldsymbol{\eta}} = \frac{\partial E_\eta}{\partial \boldsymbol{\eta}} (\boldsymbol{\omega}(\boldsymbol{\eta}) + \mathbf{h}(\boldsymbol{\eta}, \mathbf{z}) + \boldsymbol{\rho}(\boldsymbol{\eta})\mathbf{v}) \\ &= L_\omega E_\eta + L_h E_\eta + L_{\rho_1} E_\eta v_1 + L_{\rho_2} E_\eta v_2. \end{aligned} \quad (14)$$

The following calculation shows that $L_\omega E_\eta = 0$,

$$\begin{aligned} L_\omega E_\eta &= \frac{\partial E_\eta}{\partial \boldsymbol{\eta}} \boldsymbol{\omega}(\boldsymbol{\eta}) = \frac{1}{2}\dot{\mathbf{q}}_u^\top \left(\frac{\partial \mathbf{M}_{11}(\mathbf{q})}{\partial \mathbf{q}_u} \dot{\mathbf{q}}_u \right) \dot{\mathbf{q}}_u + G_u(\mathbf{q})^\top \dot{\mathbf{q}}_u \\ &\quad - \dot{\mathbf{q}}_u^\top \mathbf{M}_{11} \mathbf{M}_{11}^{-1} (G_u(\mathbf{q}) + \tilde{C}_u(\mathbf{q}, \dot{\mathbf{q}}_u)\dot{\mathbf{q}}_u) = 0 \end{aligned}$$

since $\frac{1}{2}((\partial \mathbf{M}_{11}(\mathbf{q})/\partial \mathbf{q}_u)\dot{\mathbf{q}}_u) - \tilde{C}_u(\mathbf{q}, \dot{\mathbf{q}}_u)$ is skew-symmetric and appears in a quadratic expression. Hence, $E_\eta = L_h E_\eta + L_\rho E_\eta v$, where $L_\rho E_\eta = (L_{\rho_1} E_\eta, L_{\rho_2} E_\eta)$. The term $L_h E_\eta$ in (14) vanishes when $\mathbf{z} = \dot{\mathbf{q}}_a = 0$. It is easy to verify that

$$L_\rho E_\eta = -\dot{\mathbf{q}}_u^T \mathbf{M}_{11} \mathbf{M}_{11}^{-1} \mathbf{M}_{12} = -\mathbf{M}_{12} \dot{\mathbf{q}}_u^T.$$

It is now possible to attempt the local passivation of the parallel interconnection (12,13) in two ways, leading to the same zero dynamics analyses but different design conditions.

3.2.1 Direct passivity based approach

A double integrator sub-system (13) is passive for any output of the form $\mathbf{y}_z = \mathbf{C}\mathbf{z} = (\mathbf{0}; \mathbf{K}_2)\mathbf{z}$, $\mathbf{K}_2 > 0$, with a storage function $S_1 = \frac{1}{2}\mathbf{z}^T \mathbf{Q}_1 \mathbf{z}$, as it is readily verified that $\Phi^T \mathbf{Q}_1 + \mathbf{Q}_1 \Phi = \mathbf{0}$ for $\mathbf{Q}_1 = (\mathbf{0}; \mathbf{0}, \mathbf{0}; \mathbf{K}_2) \geq 0$ while $\mathbf{B}^T \mathbf{Q}_1 = \mathbf{C}$. Such an input-output system is however not zero state detectable since $\mathbf{y}_z \equiv \mathbf{0}$ does not imply that $\mathbf{z}_1 \equiv \mathbf{0}$. A possible ‘‘energy shaping’’ output function for the nonlinear sub-system is

$$\mathbf{y}_\eta \triangleq (E_\eta - V_{\max}) L_\rho E_\eta$$

in which V_{\max} is the largest potential energy of the system at the unstable equilibrium. If not for the presence of the term $\mathbf{h}(\boldsymbol{\eta}, \mathbf{z})$ in (12), the corresponding storage function for the nonlinear sub-system would be given by,

$$S_\eta(\boldsymbol{\eta}) \triangleq \frac{1}{2}(E_\eta - V_{\max})^2,$$

as then

$$\begin{aligned} \dot{S}_\eta &= (E_\eta - V_{\max}) \dot{E}_\eta = (E_\eta - V_{\max}) L_h E_\eta + (E_\eta - V_{\max}) L_\rho E_\eta v \\ &= (E_\eta - V_{\max}) L_h E_\eta + \mathbf{y}_\eta v. \end{aligned}$$

The presence of the term associated with $L_h E_\eta$ is an obstacle to the design of a passivity-based stabilizing controller since setting $\mathbf{v} = -\mathbf{K}_3 y_\eta^T$; $\mathbf{K}_3 > 0$ does not immediately ensures that $\dot{S}_\eta \leq 0$ at all times. It is useful to investigate the rate of change of the storage function for the parallel interconnection of the linear and nonlinear sub-systems in the hope that the lack of passivity in the nonlinear sub-system can be compensated by passivity in the linear sub-system. The storage function for the parallel interconnection is the sum of the storage functions for the individual sub-systems:

$$S(\mathbf{z}, \boldsymbol{\eta}) = S_1(\mathbf{z}) + S_\eta(\boldsymbol{\eta}).$$

Thus,

$$\begin{aligned}
\dot{S}(\mathbf{z}, \boldsymbol{\eta}) &= \frac{1}{2}[\dot{\mathbf{z}}^\top \mathbf{Q}_1 \mathbf{z} + \mathbf{z}^\top \mathbf{Q}_1 \dot{\mathbf{z}}] + [E_\eta - V_{\max}] \dot{E}_\eta \\
&= \frac{1}{2} \mathbf{v}^\top \boldsymbol{\Psi}^\top \mathbf{Q}_1 \mathbf{z} + \frac{1}{2} \mathbf{z}^\top \mathbf{Q}_1 \boldsymbol{\Psi} \mathbf{v} + [E_\eta - V_{\max}] L_h E_\eta + \mathbf{y}_\eta \mathbf{v} \\
&= \mathbf{y}_z \mathbf{v} + \mathbf{y}_\eta \mathbf{v} + [E_\eta - V_{\max}] L_h E_\eta.
\end{aligned}$$

Setting

$$\mathbf{v} \triangleq -\mathbf{K}_3[\mathbf{y}_z + \mathbf{y}_\eta]^\top = -\mathbf{K}_3 \mathbf{K}_2 \dot{\mathbf{q}}_a - [E_\eta - V_{\max}] \mathbf{K}_3 L_\rho E_\eta, \quad (15)$$

yields

$$\dot{S}(\mathbf{z}, \boldsymbol{\eta}) = -[\mathbf{y}_z + \mathbf{y}_\eta] \mathbf{K}_3 [\mathbf{y}_z + \mathbf{y}_\eta]^\top + [E_\eta - V_{\max}] L_h E_\eta. \quad (16)$$

For the parallel interconnection to be passive one should have $\dot{S} \leq 0$ in some neighborhood of the desired equilibrium. The two terms in (16) contain quadratic as well as linear terms in $\dot{\mathbf{q}}_a$. These terms have to be balanced so that $\dot{S} \leq 0$ by adequate selection of the gains \mathbf{K}_2 and \mathbf{K}_3 while the gain \mathbf{K}_3 must be positive definite and bounded, and could be state dependent, if necessary. The following assumption is made to ensure the passivity of the parallel connection.

Assumption 1. *There exist gain matrices $\mathbf{K}_2 > 0$, $\mathbf{K}_3 > 0$ such that in some neighborhood $\Omega \subset \mathbb{R}^8$ of the unstable equilibrium, for some constant $c > 0$,*

$$\dot{S}(\mathbf{z}, \boldsymbol{\eta}) \leq -c[\mathbf{y}_z + \mathbf{y}_\eta][\mathbf{y}_z + \mathbf{y}_\eta]^\top. \quad (17)$$

The zero dynamics of the system with control (15) is obtained by observing that if $\dot{S}(\mathbf{z}, \boldsymbol{\eta}) \equiv 0$ then $\mathbf{v} \equiv 0$ so that the equations of motion reduce to

$$\dot{\boldsymbol{\eta}} = \boldsymbol{\omega}(\boldsymbol{\eta}), \quad \begin{pmatrix} \dot{z}_1 \\ \dot{z}_2 \end{pmatrix} = \begin{pmatrix} z_2 \\ \mathbf{0} \end{pmatrix}.$$

since $\mathbf{h}(\boldsymbol{\eta}, \mathbf{z}) \equiv \mathbf{0}$ due to $\mathbf{z}_2 \equiv \mathbf{0}$. The latter follows from the fact that $\mathbf{z}_2 \equiv \text{const} \neq 0$ is impossible in free fall: when $\mathbf{v} \equiv 0$ the machine moves only under the action of the gravity field. It follows that also $\mathbf{q}_a \equiv \text{const}$, and that $\mathbf{y}_z \equiv \mathbf{0}$ so $\mathbf{y}_\eta \equiv \mathbf{0}$ for all times. Based on rigid body momentum considerations it can then be shown that:

Proposition 1. *The zero dynamics of the system with control (15) is the dynamics of the system moving only under the gravitational forces (since $\mathbf{v} \equiv \mathbf{0}$). The trajectories can only exhibit three types of ω -limit sets:*

1. $\{\mathbf{0}; \mathbf{0}\}$ — the unstable equilibrium point,
2. $\{\mathbf{q}_{\text{down}}; \mathbf{0}\}$ — the stable equilibrium point,
3. periodic trajectories where the system rotates in the vertical plane such that $\mathbf{q}_a \equiv 0$ at all times.

The downward equilibrium is the only undesirable ω -limit point which must be avoided and which clearly restricts the region of convergence of the swing-up controller. In view of the above discussion it then follows that

Theorem 1. *Let $\epsilon > 0$ be such that $B(\mathbf{0}; \epsilon)$ is contained in the region of attraction of a LQR controller and let the gain matrices $\mathbf{K}_2, \mathbf{K}_3 > 0$ be such that (17) holds in some set Ω which contains $B(\mathbf{0}; \epsilon)$. Then every trajectory of the system with the swing-up controller that starts and remains in Ω eventually enters $B(\mathbf{0}; \epsilon)$ where the LQR controller stabilizes the system asymptotically to the unstable equilibrium. The hybrid control employing these gains is hence stabilizing the system with region of convergence Ω .*

3.2.2 Passivity based approach with pre-compensation.

Prior to passivation of the parallel interconnection, the linear sub-system (13) can first be made asymptotically stable (therefore passive) by introducing a feedback transformation

$$\mathbf{v} = -\mathbf{K}_1 \mathbf{q}_a - \mathbf{K}_2 \dot{\mathbf{q}}_a + \mathbf{u}, \quad \text{with } \mathbf{K}_1 > 0, \mathbf{K}_2 > 0,$$

leading to a parallel interconnection with the new control variable \mathbf{u} :

$$\begin{aligned} \dot{\boldsymbol{\eta}} &= \boldsymbol{\omega}(\boldsymbol{\eta}) + \mathbf{h}(\boldsymbol{\eta}, \mathbf{z}_2) - \boldsymbol{\rho}(\boldsymbol{\eta})(\mathbf{K}_1 \mathbf{q}_a + \mathbf{K}_2 \dot{\mathbf{q}}_a) + \boldsymbol{\rho}(\boldsymbol{\eta})\mathbf{u}, \\ \dot{\mathbf{z}} &= (\tilde{\boldsymbol{\Phi}} - \tilde{\boldsymbol{\Psi}}(\mathbf{K}_1; \mathbf{K}_2))\mathbf{z} + \tilde{\boldsymbol{\Psi}}\mathbf{u}, \end{aligned}$$

where the linearized sub-system is equivalent to two periodic systems (double oscillator) with state space matrices $\tilde{\boldsymbol{\Phi}} = \begin{pmatrix} \mathbf{0} & \mathbf{I} \\ -\mathbf{K}_1 & -\mathbf{K}_2 \end{pmatrix}$, $\tilde{\boldsymbol{\Psi}} = (\mathbf{0} \ \mathbf{I})$.

An output of the form $\mathbf{y}_2 = [\mathbf{Q}_{12}^T; \mathbf{Q}_{22}] \mathbf{z}$, renders the linear sub-system passive, this time, for a strictly positive definite matrix $\mathbf{Q}_2 > 0$, satisfying

$$\tilde{\boldsymbol{\Phi}}^T \mathbf{Q}_2 + \mathbf{Q}_2 \tilde{\boldsymbol{\Phi}} < 0; \quad \tilde{\boldsymbol{\Psi}}^T \mathbf{Q}_2 = [\mathbf{Q}_{12}^T; \mathbf{Q}_{22}].$$

Clearly, one such matrix \mathbf{Q}_2 is of the form

$$\mathbf{Q}_2 = \begin{pmatrix} \mathbf{Q}_{11} & \mathbf{Q}_{12} \\ \mathbf{Q}_{12}^T & \mathbf{Q}_{22} \end{pmatrix}.$$

The quadratic form $S_2(\mathbf{z}) = \frac{1}{2} \mathbf{z}^T \mathbf{Q}_2 \mathbf{z}$ then obviously satisfies,

$$\dot{S}_2 \leq \mathbf{y}_2 \mathbf{u}.$$

and hence is a storage function for the linear sub-system. The bound for the rate of change in the storage function for the parallel connection, $S \triangleq S_2 + S_\eta$, while employing the same output \mathbf{y}_η and storage function S_η for the nonlinear

sub-system as before, is now:

$$\begin{aligned}\dot{S}(\mathbf{z}, \boldsymbol{\eta}) &= \frac{1}{2}[\dot{\mathbf{z}}^\top \mathbf{Q}_2 \mathbf{z} + \mathbf{z}^\top \mathbf{Q}_2 \dot{\mathbf{z}}] + (E_\eta - V_{\max})\dot{E}_\eta \\ &= \frac{1}{2}\mathbf{u}^\top \boldsymbol{\Psi}^\top \mathbf{Q}_2 \mathbf{z} + \frac{1}{2}\mathbf{z}^\top \mathbf{Q}_2 \boldsymbol{\Psi} \mathbf{u} \\ &\quad + (E_\eta - V_{\max})(L_h E_\eta - L_\rho E_\eta \mathbf{K}_1 \mathbf{q}_a - L_\rho E_\eta \mathbf{K}_2 \dot{\mathbf{q}}_a) + \mathbf{y}_\eta \mathbf{u} \\ &= \mathbf{y}_z \mathbf{u} + \mathbf{y}_\eta \mathbf{u} + (E_\eta - V_{\max})(L_h E_\eta - L_\rho E_\eta \mathbf{K}_1 \mathbf{q}_a - L_\rho E_\eta \mathbf{K}_2 \dot{\mathbf{q}}_a).\end{aligned}$$

Selecting the swing-up control \mathbf{u} as before while remembering about the pre-compensation yields

$$\begin{aligned}\mathbf{v} &\triangleq -\mathbf{K}_1 \mathbf{q}_a - \mathbf{K}_2 \dot{\mathbf{q}}_a - \mathbf{K}_3 (\mathbf{y}_z + \mathbf{y}_\eta)^\top \\ &= -\mathbf{K}_1 \mathbf{q}_a - \mathbf{K}_2 \dot{\mathbf{q}}_a - \mathbf{K}_3 \mathbf{Q}_{12}^\top \mathbf{q}_a - \mathbf{K}_3 \mathbf{Q}_{22} \dot{\mathbf{q}}_a - (E_\eta - V_{\max}) \mathbf{K}_3 L_\rho E_\eta.\end{aligned}\quad (18)$$

Hence, the new bound becomes

$$\dot{S}(\mathbf{z}, \boldsymbol{\eta}) = -(\mathbf{y}_z + \mathbf{y}_\eta) \mathbf{K}_3 (\mathbf{y}_z + \mathbf{y}_\eta)^\top + (E_\eta - V_{\max})(L_h E_\eta - L_\rho E_\eta \mathbf{K}_1 \mathbf{q}_a - L_\rho E_\eta \mathbf{K}_2 \dot{\mathbf{q}}_a).$$

The counterpart of Assumption 1 is needed.

Assumption 2. *There exist gain matrices $\mathbf{K}_1 > 0$, $\mathbf{K}_2 > 0$ and $\mathbf{K}_3 > 0$ such that in some neighborhood $\Omega \subset \mathbb{R}^8$ of the unstable equilibrium, for some constant $c > 0$*

$$\dot{S}(\mathbf{z}, \boldsymbol{\eta}) \leq -c(\mathbf{y}_z + \mathbf{y}_\eta)(\mathbf{y}_z + \mathbf{y}_\eta)^\top.\quad (19)$$

It should be noted that the gains must satisfy: $-\mathbf{K}_1 - \mathbf{K}_3 \mathbf{Q}_{12}^\top < 0$ and $-\mathbf{K}_2 - \mathbf{K}_3 \mathbf{Q}_{22} < 0$. Only the first inequality requires attention since $\mathbf{Q}_{12} < 0$. The zero dynamics of the system with control (18) is obtained by observing that if $\dot{S}(\mathbf{z}, \boldsymbol{\eta}) \equiv 0$ then $\mathbf{v} \equiv \mathbf{0}$ so that the equations of motion reduce to

$$\begin{aligned}\dot{\boldsymbol{\eta}} &= \boldsymbol{\omega}(\boldsymbol{\eta}) + \mathbf{h}(\boldsymbol{\eta}, \mathbf{z}_2), \\ \begin{pmatrix} \dot{\mathbf{z}}_1 \\ \dot{\mathbf{z}}_2 \end{pmatrix} &= \begin{pmatrix} \mathbf{z}_2 \\ -\mathbf{K}_1 \mathbf{z}_1 - \mathbf{K}_2 \mathbf{z}_2 \end{pmatrix}.\end{aligned}$$

Clearly, $\mathbf{z}_1 \rightarrow \mathbf{0}$ and $\mathbf{z}_2 \rightarrow \mathbf{0}$ since \mathbf{K}_1 and \mathbf{K}_2 are stabilizing for the linearized sub-system. It follows that $\mathbf{h}(\boldsymbol{\eta}, \mathbf{z}_2) \rightarrow 0$ which implies that the zero dynamics is reduced to

$$\dot{\boldsymbol{\eta}} = \boldsymbol{\omega}(\boldsymbol{\eta}), \quad \mathbf{z}_1 \equiv \mathbf{0}, \quad \mathbf{z}_2 \equiv \mathbf{0}.$$

Since the zero dynamics is also equivalent to the system moving under the sole action of gravity, Proposition 1 still holds. Like before, the downward equilibrium is the only undesirable ω -limit point which must be avoided. It follows that

Theorem 2. *Let $\epsilon > 0$ be such that $B(\mathbf{0}; \epsilon)$ is contained in the region of attraction of a LQR controller and let the gain matrices $\mathbf{K}_1, \mathbf{K}_2, \mathbf{K}_3 > 0$ be such that (19) holds in some set Ω which contains $B(\mathbf{0}; \epsilon)$, then every trajectory of the system with the swing-up controller that starts and remains*

in Ω eventually enters $B(\mathbf{0}; \epsilon)$ where the LQR controller stabilizes the system asymptotically to the unstable equilibrium. The hybrid control employing these gains is hence stabilizing the system with region of convergence Ω .

The passivity approach with pre-compensation enjoys advantages compared to the un-compensated approach. The zero dynamics is easier to isolate and $S_2 \rightarrow 0$ so that $S \rightarrow \frac{1}{2}E_\eta^2 \equiv \text{const}$. The latter delivers a simple criterion by which to tune the controller gains. It is also possible to consider a non-smooth output function $\mathbf{y}_\eta \triangleq |E_\eta - V_{\max}|L_\rho E_\eta$ leading to the controller

$$\mathbf{v} \triangleq -\mathbf{K}_1 \mathbf{q}_a - \mathbf{K}_3 \mathbf{K}_2 \dot{\mathbf{q}}_a - |E_\eta - V_{\max}| \mathbf{K}_3 L_\rho E_\eta \quad (20)$$

3.3 Simulation results

The switching algorithm between the two controllers is designed as follows.

1. Activate swing-up controller (20);
2. If $V_{\max} + L(\mathbf{q}, \dot{\mathbf{q}}) < 3\%V_{\max}$, switch to 4;
3. If $V_{\max} + L(\mathbf{q}, \dot{\mathbf{q}}) > 10\%V_{\max}$, switch to 1;
4. Employ LQR to upright position.

where $L(\mathbf{q}, \dot{\mathbf{q}})$ is the Lagrangian (1) of the system. For the balance phase, the parameters of the LQR controller are as in in Section 3.1. In Example 8 the initial conditions were $\mathbf{q}_0 = [10^\circ, -10^\circ, -30^\circ, 30^\circ]^\top$, $\dot{\mathbf{q}}_0 = \mathbf{0}$. The following parameters were employed,

$$\mathbf{K}_2 \mathbf{K}_3 = \begin{pmatrix} 20 & 0 \\ 0 & 20 \end{pmatrix}, \quad \mathbf{K}_1 = \begin{pmatrix} 100 & 0 \\ 0 & 100 \end{pmatrix}, \quad \mathbf{K}_3 = \begin{pmatrix} 1 & 0 \\ 0 & 1 \end{pmatrix}.$$

As shown in Fig. 3a below, the controller switches at $t = 0.182$ s, and the system stabilizes to its unstable equilibrium configuration in about 6 seconds. In Example 9 the initial condition is $\mathbf{q}_0 = [30^\circ, 10^\circ, -135^\circ, -20^\circ]^\top$, $\dot{\mathbf{q}}_0 = \mathbf{0}$ which is very far from the unstable equilibrium. The following parameters for the swing-up controller were successful,

$$\mathbf{K}_2 \mathbf{K}_3 = \begin{pmatrix} 8 & 0 \\ 0 & 8 \end{pmatrix}, \quad \mathbf{K}_1 = \begin{pmatrix} 16 & 0 \\ 0 & 16 \end{pmatrix}, \quad \mathbf{K}_3 = \begin{pmatrix} 2.1 & 0 \\ 0 & 2.1 \end{pmatrix}.$$

The controller switches at $t = 0.688$ s, and the system stabilizes in about 2 seconds. Its trajectories are shown in Fig. 3f below. The hybrid algorithm provides for a much larger ROC but one of the difficulties in applying the passivity approach is to have to tune the parameters.

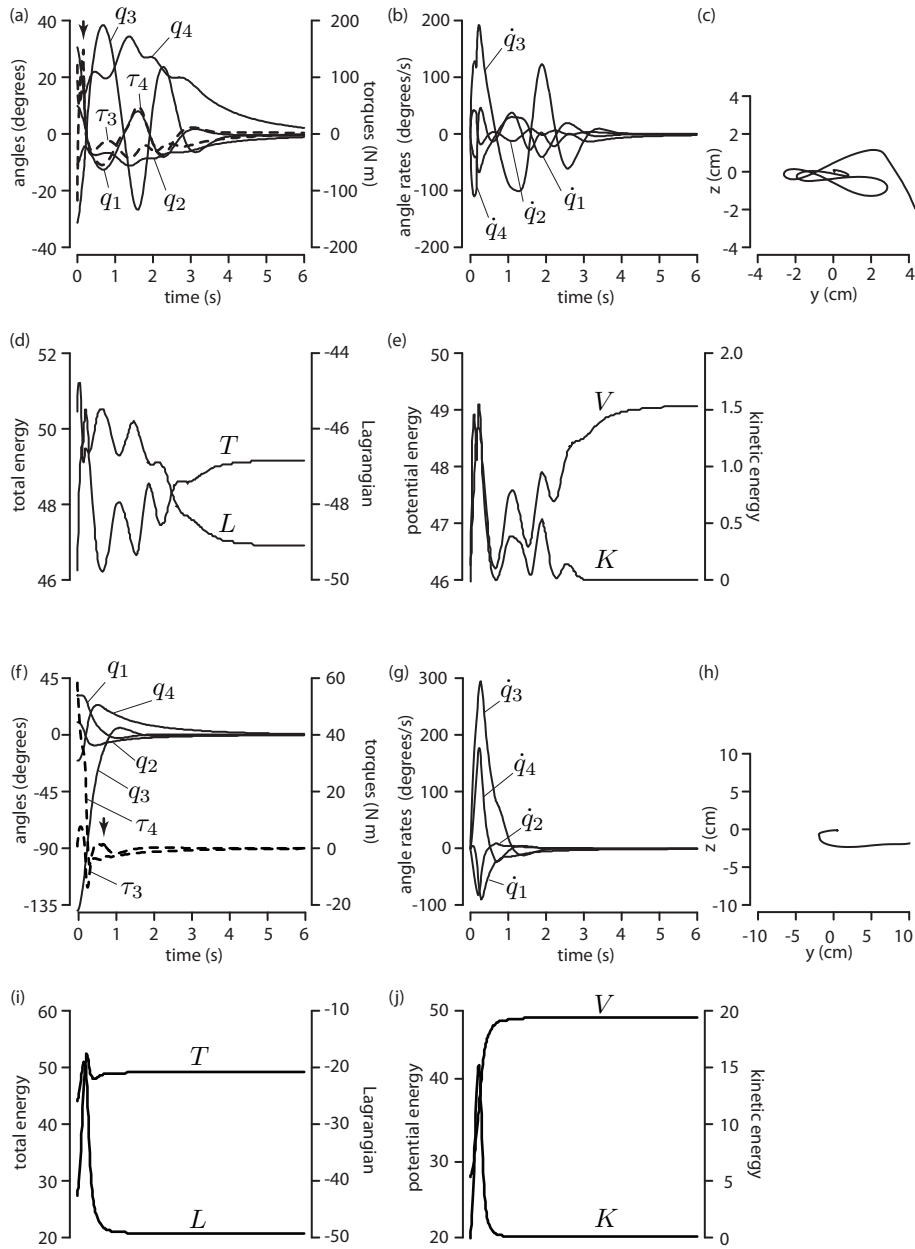


Fig. 3 Examples 8 and 9. (a,f): Joint angles and torques. Arrows shows where the controller switches. (b,g): Joint velocities. (c,h): Stabilograms of COM projected on the ground. (d,i): Total energy and Lagrangian. (e,j): Potential and kinetic Energy.

4 Conclusion

We have employed a passivity-based approach to stabilize the spatial double inverted pendulum actuated at the hip that can be viewed as a model of standing creatures. An energy-shaping control could be found with proper design of a storage function, by-passing the solution of the energy shaping equations. Such approach was more effective if the system was partially linearized by pre-compensation. The controller has a swing-up phase, applicable to a large set of initial conditions, that drives the system to a small neighborhood of the unstable equilibrium where a linear controller can regulate the system near the unstable equilibrium thanks to its robustness properties. A shortcoming of the present method is the necessity to design the controller gains. Enforcing control constraints such as limiting the maximum joint torques is also difficult. We are currently investigating a number of other nonlinear control approaches that would be applicable to systems with larger numbers of degrees of freedom.

References

1. M. W. Spong and L. Praly, Control of Underactuated Mechanical Systems Using Switching And Saturation. In *Control Using Logic-Based Switching*, A. S. Morse (Ed.), LNCIS 222, Springer-Verlag, London, pp. 162–172, 1997.
2. M. W. Spong, Underactuated Mechanical Systems. In *Control Problems in Robotics and Automation*, B. Siciliano and K. P. Valavanis (Eds.), LNCIS 230, Springer-Verlag, London, pp. 135–150, 1998.
3. Xinjilefu, V. Hayward, and H. Michalska, Stabilization of the Spatial Double Inverted Pendulum Using Stochastic Programming Seen as a Model of Standing Postural Control, Proc. *9th IEEE-RAS Int. Conf. on Humanoid Robots*, pp. 367–372, 2009.
4. M. Murray, Z. Li, Z., and S. S. Sastry, *A Mathematical Introduction to Robotic Manipulation*. CRC Press, Boca Raton, 1994.
5. J. E. Marsden and T. S. Ratiu, *Introduction to Mechanics and Symmetry: A Basic Exposition of Classical Mechanical Systems*, Second Edition, Springer-Verlag, 1999.
6. G. Oriolo and Y. Nakamura, Control of Mechanical Systems with Second-order Nonholonomic Constraints: Underactuated Manipulators”, Proc. *30th IEEE Conference on Decision and Control*, pp. 2398–2403, 1991.
7. K. Y. Wichlund, O. J. Sordalen, O. Egeland, Control of Vehicles with Second-order Nonholonomic Constraints: Underactuated Vehicles,” Proc. *3rd European Control Conference*, pp. 3086–3091, 1995.
8. O. Ayoub, *Robotic Model of the Human Standing Posture*, M.Eng. Thesis, Department of Electrical and Computer Engineering, McGill University, 2005.
9. G. Sood, *Simulation and Control of a Hip Actuated Robotic Model for the Study of Human Standing Posture*, M.Eng. Thesis, Department of Electrical and Computer Engineering, McGill University, 2008.
10. M. Reyhanoglu, A. van der Schaft, N. H. McClamroch, and I. Kolmanovsky, Dynamics and Control of a Class of Underactuated Mechanical Systems”, *IEEE Transactions on Automatic Control*, Vol. 44, No. 9, pp. 1663–1671, 1999.
11. M. W. Spong, Swing Up Control of the Acrobot, Proc. *IEEE Int. Conf. on Robotics and Automation*, pp. 2356–2361, 1994.